Environmental Technology & Innovation 11 (2018) 105–115

Contents lists available at ScienceDirect

Environmental Technology & Innovation

journal homepage: www.elsevier.com/locate/eti

Aluminum biosorption using non-viable biomass of *Pseudomonas putida* immobilized in agar–agar: Performance in batch and in fixed-bed column

Paola S. Boeris, Andrés S. Liffourrena, Gloria I. Lucchesi *

Departamento de Biología Molecular. Facultad de Ciencias Exactas, Físico-Químicas y Naturales, Universidad Nacional de Río Cuarto, Río Cuarto, Córdoba, Argentina

HIGHLIGHTS

- Al^{3+} adsorption by non-living *P. putida* trapped in agar in batch and fixed-bed column.
- Biosorption capacity was higher in fixed-bed column than in batch experiments.
- Fixed-bed column was stable up to 12 successive adsorption/desorption cycles.
- Fixed-bed is a very good alternative for the removal of Al^{3+} from aqueous solutions.

GRAPHICAL ABSTRACT

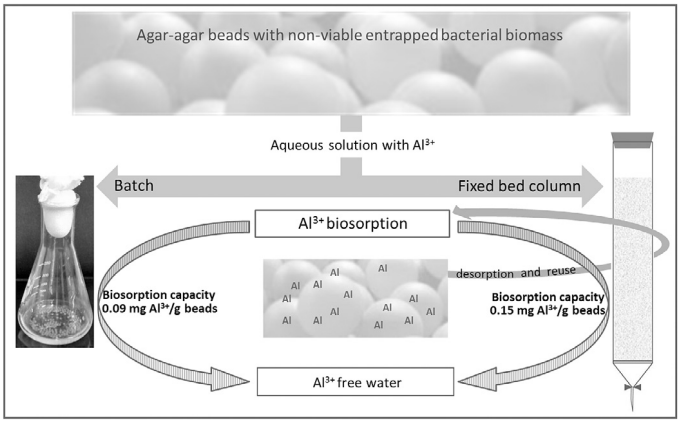

ARTICLE INFO

Article history:
Received 19 January 2018
Received in revised form 20 April 2018
Accepted 10 May 2018
Available online 17 May 2018

Keywords:
Aluminum
Adsorption
P. putida
Fixed-bed column

ABSTRACT

Non-viable biomass of *Pseudomonas putida* immobilized in agar–agar was used as adsorbent to remove aluminum from aqueous solutions. In batch assays, adsorption equilibrium was reached after 45 min and 95% of 2.7 mg/L Al^{3+} were adsorbed. Immobilized biomass was packed to obtain a fixed-bed column and the dynamic behavior in continuous mode was established through breakthrough curves. At different flow rates (0.5 and 1.0 mL/min) the adsorption capacity of the column did not change, but removal percentage was higher at the lowest flow rate (64.92% and 44.34%, respectively). The fixed-bed column presented a higher biosorption capacity than that obtained in batch experiments (0.15 and 0.09 mg Al^{3+}/g beads, respectively), and showed stability for up to 12 successive adsorption/desorption cycles with negligible loss in adsorption efficiency. We concluded

* Correspondence to: Departamento de Biología Molecular, Facultad de Ciencias Exactas Físico-Químicas y Naturales, Universidad Nacional de Río Cuarto, CPX5804BYA Río Cuarto. Córdoba, Argentina.
E-mail address: glucchesi@exa.unrc.edu.ar (G.I. Lucchesi).

https://doi.org/10.1016/j.eti.2018.05.003

that this packed biosorbent could be a good alternative for the removal of Al^{3+} from aqueous solutions.

1. Introduction

At present, pollution by metal ions is a major environmental problem. Aluminum is generally complexed with minerals and inaccessible to living systems, but the advance of industrialization, linked to acid rain and a decrease in soil pH, has increased the leaching of the metal in groundwater (Tharmalingam et al., 2007 and citations therein; Auger et al., 2013), with a prevalence of harmful soluble species, such as the Al^{3+} cation (Garcidueñas Piña and Cervantes, 1996). It has also been described that the indiscriminate use of chemical fertilizers and agrochemicals causes acidification of soils, which leads to an increase in those aluminum forms that are toxic for plant growth (Kochian et al., 2005; Sukweenadhi et al., 2015).

Aluminum has been detected in drinking water (Kumari and Ravindhranath, 2012) and in effluents from a wide variety of industries, where it is used as raw material or as a component of final products (for e.g. in the manufacturing of packaging materials and domestic utensils, aeronautics, automobiles, pharmaceutical and medicine products) (Soylak et al., 1997; de Amorim et al., 2006; Tuzen and Soylak, 2008; Tassist et al., 2010). The aquatic toxicity of aluminum is strongly influenced by the species of metal, which in turn depends on the pH value of the solution. At pH values close to 4, most aluminum exists as free Al^{3+}, while at pH values greater than 7, insoluble hydroxylated forms are present (Garcidueñas Piña and Cervantes, 1996). Relatively insoluble aluminum hydroxy species tend to be less biologically available, and as a consequence, significantly less toxic than monomeric species or free metal ions (Dixon, 1997).

For a long time, Al^{3+} was considered harmless for living organisms. However, several studies have since shown its harmful effects (Mailloux et al., 2011; Tomljenovic, 2011). Particularly in humans, the accumulation of this metal in the brain has been related to neurodegenerative diseases such as Alzheimer's, Parkinson's and amyotrophic lateral sclerosis (Wong et al., 1998; Buratti et al., 2006). In plants, Al^{3+} released into the soil limits root growth and activates oxidative stress, leading to structural cell damage, lack of growth and lack of root development (Singh et al., 2017).

Metals are non-biodegradable species and their removal from wastewater can be carried out through various methods. Physico-chemical methods (ion exchange, chemical precipitation, electroflotation, osmosis) have several disadvantages: they need chemical additives, have a high energy requirement and a high operating cost, do not completely remove the metal, and produce toxic sludge and secondary pollution (Mittal et al., 2010; Gupta and Nayak, 2012; Devaraj et al., 2016). Compared to conventional techniques, biosorption is a potential alternative for toxic metal removal since it is an eco-friendly, efficient process that allows the removal of metal traces (Loutseti et al., 2009; Majumder et al., 2015; Abdolali et al., 2015; Rashid et al., 2016; Muñoz et al., 2016, Boeris et al., 2016; Zang et al., 2017; Muñoz et al., 2017; Barquilha et al., 2017; Abdolali et al., 2017). With biosorption, metals bind to different ligands present on the surfaces of biological materials (carboxyl, phosphate, amine, imidazel, thioether, sulfhydryl and hydroxyl groups). Biosorbents can be metabolically active or inactive biomasses of algae, fungi, yeast and bacteria, as well as industrial and agricultural wastes (Vijayaraghavan and Yun, 2008; Wang and Chen, 2009). When bacterial biomass is used as adsorbent, biosorption can be carried out with microorganisms in free condition (planktonic state) or immobilized in polymeric matrices (Vijayaraghavan and Yun, 2008). The use of immobilized biomass as an adsorbent has a number of advantages, such as its easy extraction from the effluent to be treated, its operational flexibility, its reusability, and its low operating costs. Additionally, the immobilized adsorbent can be packed in glass or PVC columns to create fixed-bed reactors (Vijayaraghavan and Yun, 2008; Majumder et al., 2015; Muñoz et al., 2016; Zang et al., 2017; Barquilha et al., 2017; Abdolali et al., 2017; Dhoble et al., 2017). The use of these columns allows continuous flow operations with high pollutant removal efficiency. Furthermore, the process can be scaled from a laboratory scale to a full or industrial scale (Vijayaraghavan and Yun, 2008; Barquilha et al., 2017).

In a previous study we demonstrated that metabolically active and inactive biomass of *Pseudomonas putida* A (ATCC 12633) is able to attach to Al^{3+}. Scanning electron microscopy (SEM) photomicrographs of non-living biomass exposed to Al^{3+} showed the presence of particles in the form of an irregular globule on the cell surface, indicative of the presence of metal. Moreover, by infrared spectroscopy analysis it was determined that the metal is adsorbed to amine, hydroxyl and phosphate groups on the cell surface, with the phosphatidylcholine content of the bacterial membrane being particularly important for adsorption capacity (Boeris and Lucchesi, 2012; Boeris et al., 2016). Using both biomass types, Al^{3+} adsorption was fast and stable in time, and efficient at pH 4.3 between 15 and 42 °C. However, non-viable biomass showed higher adsorption capacity than that determined for viable biomass (0.55 and 0.48 mg Al^{3+}/g adsorbent, respectively) (Boeris et al., 2016). The greater adsorption capacity of non-viable biomass was attributed to the fact that this biomass was obtained by autoclaving and, accordingly, the cells provided a larger available surface area and more surface binding sites (Errasquin and Vazquez, 2003).

Given the biosorption abilities of *P. putida* A (ATCC 12633) biomass in regards to aluminum ions, and the possible advantages offered by biomass immobilization to improve the biosorption process, in this study we evaluated Al^{3+} biosorption in batch experiments using non-viable *P. putida* biomass immobilized in agar–agar beads. Also, for the purpose of evaluating the biosorption process in continuous mode, a fixed-bed column was designed and the factors influencing its performance were analyzed.

2. Materials and methods

2.1. Reagents, microorganisms and culture conditions

All reagents used in this study were analytical-grade. The stock solution of Al^{3+} (as $AlCl_3$) (Merk) was prepared at 1000 mg/L in distilled water.

The collection strain *Pseudomonas putida* A (ATCC 12633) (Palleroni, 1992) was grown aerobically at 30 °C for 14–16 h with shaking in Luria–Bertani (LB) medium until late exponential phase (OD_{660} 0.8–1.00). Growth was measured by the absorbance of the culture at 660 nm (Beckman DU 640 spectrophotometer).

2.2. Al^{3+} quantification

Free Al^{3+} was measured through the colorimetric method described by Hejri et al. (2011). This method allows the determination of trace amounts of aluminum (quantification limits: 0.2 ng/mL), and it is based on the formation of the colored Al^{3+}-Eriochromecyanine R complex and the subsequent extraction of the complex with Br-cetyltrimethylammonium (CTAB). The absorbance of the complex obtained was measured at 595 nm with a spectrophotometer (Beckman DU 640).

2.3. Biosorbent preparation

P. putida A (ATCC 12633), grown as previously described, was inactivated by heat (autoclaved at 121 °C, 1.2 atm for 30 min). The non-viable biomass was harvested by centrifugation in a Sorvall RC5C refrigerated centrifuge (8000 × g for 10 min at 4 °C), washed with deionized water and lyophilized. The non-viable biomass was stored at 4 °C and used for further studies. Following this procedure, approximately 800 mg of lyophilized biomass were obtained per liter of culture.

2.4. Preparation of agar–agar beads with immobilized biomass

2% w/v of agar–agar and 0.5% w/v of non-viable lyophilized biomass were mixed and dissolved in deionized water. The suspension was dripped into cold vegetable oil to favor bead gelation. The beads obtained were washed with distilled water in order to remove excess oil and non-entrapped biomass (Mokaddem et al., 2014). The beads were stored at 4 °C and used for further studies. When necessary, empty beads were obtained as described above without added biomass. Trapped biomass reached a value of about 5.5 mg biomass/g beads.

2.5. Biosorption batch assays

2.5.1. Kinetic adsorption

0.6 g beads (with and without trapped biomass) were placed in Erlenmeyer flasks containing 5 mL aqueous solution at pH 4.3 plus 2.7 mg/L Al^{3+} and incubated at 20–22 °C (room temperature) with 150 rpm agitation. At different time intervals (0, 1, 15, 30, 45, 90 and 120 min) 100 μl aliquots were taken and the free metal was quantified. The amount of metal adsorbed (q_e), expressed as mg metal/g beads or % adsorption, were calculated using Eqs. (1) and (2), respectively:

$$q_e = (Ci - Cf)V/m \tag{1}$$

$$R(\%) = (Cf - Ci)100/Cf \tag{2}$$

where Ci (mg/L): initial concentration; Cf (mg/L): final concentration; V (L): volume of the solution; m (g): amount of beads.

2.5.2. Adsorption assays

Adsorption of different initial concentrations of Al^{3+} to the beads with entrapped biomass was evaluated in batch assays. 0.15 g beads were placed in Erlenmeyer flasks containing a 5 mL aqueous solution at pH 4.3 with different Al^{3+} concentrations (from 0 to 5.4 mg/L). After 45 min incubation at room temperature, samples were taken and the free metal was quantified. The interaction between the adsorbent and Al^{3+} was analyzed using the isotherm models of Langmuir (1918) and Freundlich (1906).

The Langmuir isotherm, in its non-linear form, is described by the equation:

$$q_e = q_{\max} K_L C_e / 1 + K_L C_e$$

where q_e (mg/g): amount of metal adsorbed, C_e (mg/L): concentration of metal in liquid phase at equilibrium, $q_{\max}$ (mg/g): maximum sorption capacity and K_L (L/mg): Langmuir constant related to the affinity between the metal and the sorbent.

The Freundlich isotherm, in its non-linear form, is described by the equation:

$$q_e = K_F C_e^{1/n}$$

where K_F (L/g): Freundlich constant that represents uptake capacity, n (mg/g): constant related to adsorption intensity.

For both isotherm models, K_L and K_F are the values obtained from the slope and from the double-reciprocal plot of the saturation curve constructed by plotting q_e versus C_e. $q_{\max}$ and n are the values obtained from the intercept of the same double-reciprocal plots (Febrianto et al., 2009).

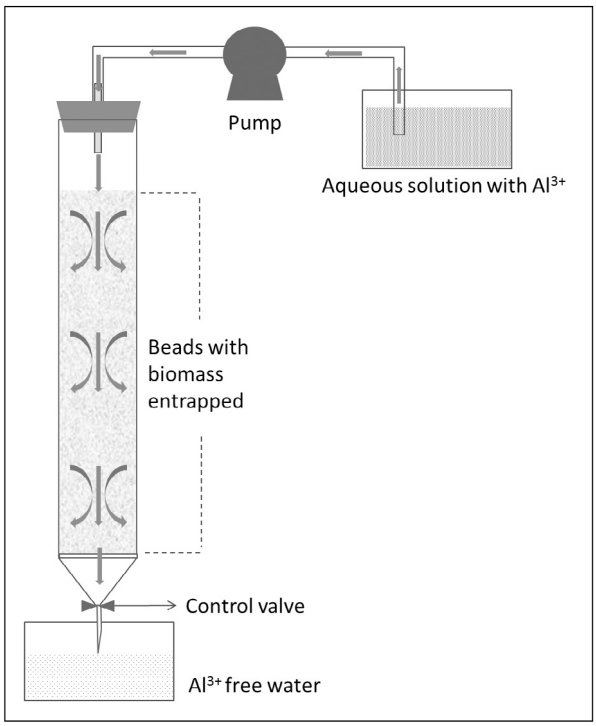

Fig. 1. Schematic diagram of the fixed bed column designed to adsorb Al^{3+}.

2.5.3. Influence of ions on the adsorption process

0.6 g beads suspended in a 5 mL aqueous solution at pH 4.3 were exposed to 2.7 mg/L Al^{3+} in presence or absence of 1.6 g/L NaCl, 1.3 g/L KCl, 2.0 g/L $CaCl_2$, 0.006 g/L NaF, 0.42 g/L KNO_3, 3.0 g/L $MgSO_4$ and 0.3 g/L $KHCO_3$. After 45 min incubation at room temperature, Al^{3+} was quantified by the colorimetric method as described above.

2.5.4. Al^{3+} desorption and reuse

The beads were subjected to successive sorption/desorption cycles. Sorption was carried out for 45 min at room temperature with 0.6 g beads suspended in a 5 mL aqueous solution at pH 4.3 containing 2.7 mg/L Al^{3+}. Desorption of bound Al^{3+} was conducted through washes of the beads with 5 mL HCl 0.01 N in an orbital shaker at 100 rpm (Boeris et al., 2016). At different time intervals (from 0 to 60 min) aliquots were taken and the desorbed metal was quantified. After each desorption step, the beads were washed with deionized water and reused for a new adsorption step.

2.6. Biosorption assays in fixed-bed column

2.6.1. Design of the fixed-bed column

The column was made using a glass tube with an inner diameter of 2 cm and a length of 37 cm. 60 g beads with non-viable entrapped biomass or beads without entrapped biomass were packed to obtain a bed depth of 25 cm (Fig. 1). Aqueous solutions at pH 4.3 with different Al^{3+} concentrations (150, 180 and 210 mg/L) were pumped through the fixed bed column using a peristaltic pump at two different flow rates (0.5 and 1 mL/min). When necessary, Al^{3+} adsorption was evaluated in presence of 1.6 g/L NaCl, 1.3 g/L KCl, 2.0 g/L $CaCl_2$, and 3.0 g/L $MgSO_4$. The amount of Al^{3+} in the effluent was quantified by the colorimetric method (Hejri et al., 2011).

2.6.2. Analysis of breakthrough curves

The fixed-bed column performance is described by means of the breakthrough curve obtained by plotting the ratio between effluent and influent Al^{3+} concentration (C_{eff}/C_{inf}) as a function of time. Different parameters were determined from the breakthrough curve, including breakthrough time (T_b), exhausting time (T_e) and biosorption capacity of the column (q_{ec}). T_b is the time at which the Al^{3+} concentration in the effluent reached 5% of the Al^{3+} concentration in the influent, and T_e is the time at which the Al^{3+} concentration in the effluent reached 95% of the Al^{3+}concentration in the influent. The biosorption capacity of the column is given by the amount of Al^{3+} per gram of adsorbent (mg Al^{3+}/g beads). The other parameters obtained from the breakthrough curves were total amount of adsorbed Al^{3+}(q_{total}), metal removal percentage (R_c%) and total amount of Al^{3+} sent to the column (me_{total}) (Muñoz et al., 2016).

2.6.3. Modeling of breakthrough curves

The mathematical models of Thomas (1948) and Yoon and Nelson (1984) were used to optimize the fixed-bed column for scaling up the adsorption process to a larger operation.

The linearized form of the Thomas model can be expressed by the equation:

$$\ln[(C_{inf}/C_{eff}) - 1] = (K_{Th}q_o m/Q) - K_{Th}C_{inf}t$$

where K_{Th} (L/mg min): Thomas kinetic constant, and q_0 (mg/g): maximum solid-phase metal concentration. The values of q_0 and K_{Th}correspond to the intercept and slope, respectively, of the linear plot $\ln[(C_{inf}/C_{eff})-1]$ versus time (Xu et al., 2013).

The linearized form of Yoon–Nelson model is expressed thus:

$$\ln[C_{inf}/(C_{inf} - C_{eff})] = K_{YN}t - \tau K_{YN}$$

where K_{YN} (min^{-1}): Yoon–Nelson kinetic constant, τ (min): time required for 50% metal breakthrough. The values of τ and K_{YN} correspond to the intercept and the slope, respectively, from the linear plot of $\ln(C_{inf}/C_{inf} - C_{eff})$ versus time.

2.6.4. Al^{3+} desorption

Metal desorption from the column was carried out with different HCl concentrations (0.1–0.01 N) and different flow rates (0.1–1 mL/min). The elution curve (equivalent to the breakthrough curve) was used to determine the elution efficiency:

$$E_d(\%) = (q_d/q_{total})100$$

where q_d is the total desorbed metal and q_{total} is the time until a residual Al^{3+}concentration in the effluent is 99% with respect to Al^{3+} bound to the column (Muñoz et al., 2016).

3. Results and discussion

3.1. Batch biosorption

3.1.1. Kinetic adsorption

The effect of contact time on the adsorption of 2.7 mg/L Al^{3+} onto beads with or without entrapped biomass is shown in Fig. 2. Metal adsorption to both bead types followed a biphasic pattern with rapid adsorption in the first 15 min. After this time, the adsorption rate decreased and reached equilibrium within 45 min. The time our study determined to be necessary for Al^{3+} to reach adsorption equilibrium was considerably lower than reported for aluminum absorption using immobilized cells of *Bacillus safensis* KTSMBNL 26 (Dhanarani et al., 2016) but similar to that reported in other studies for other metals, such as Zn^{2+} and Cu^{2+} (Loutseti et al., 2009; Rashid et al., 2016). The initially rapid adsorption of Al^{3+} to beads was likely because the binding sites of the adsorbent were available to be occupied by Al^{3+}, and the repulsive forces between the non-bonded and bonded metal were negligible. As described by Rashid et al. (2016) for the adsorption of other metals, deceleration in adsorption with an increase in contact time until equilibrium is reached can be attributed to a lower availability of binding sites and to the increase of repulsive forces. At equilibrium, adsorption capacity (q_e) of beads with non-viable trapped biomass was 0.021 mg Al^{3+}/g bead (95% adsorption), whereas the q_e of beads without biomass was approximately 10 times lower (0.0018 mg Al^{3+}/gr bead), i.e. only 11% of the metal was adsorbed (Fig. 2). These results show that although the beads without immobilized biomass have the capacity to attach to Al^{3+}, the presence of non-viable *P. putida* A (ATCC 12633) biomass notably increases the availability of binding sites for the cation. Regarding Al^{3+}, we have previously shown that phosphate, amine and hydroxyl groups on the cell surface of *P. putida* A (ATCC 12633) are major binding sites for the metal (Boeris et al., 2016). Thus, considering that the non-viable biomass was obtained after autoclaving, the highest adsorption capacity could be due to a greater number of exposed Al^{3+}-binding sites in the beads. It should be noted that the time needed to reach adsorption equilibrium onto beads (45 min) was higher than the one previously determined using free living and non-living *P. putida* A (ATCC 12633) biomass as biosorbent of Al^{3+}. For both free biosorbents, the removal of 100% of 2.7 mg/L of Al^{3+} added was achieved after 1 min Boeris et al. (2016). For immobilized biomass, the observed increase in the time required to reach adsorption equilibrium can be attributed to biomass retention within the beads, hence, mass transfer resistance is higher and this usually slows down the attainment of equilibrium (Vijayaraghavan and Yun, 2008). On the other hand, when the adsorption of 2.7 mg/L Al^{3+} onto beads was analyzed in the presence of different ions (Na^+, K^+, Ca^{2+}, Cl^-, F^-, $NO_3{}^-$, $SO_4{}^{2-}$ and $HCO_3{}^-$), metal adsorption was always higher than 85%. This indicates that at the concentrations used the ions did not significantly affect the process of adsorption to the beads (data not shown).

3.1.2. Metal–sorbent interaction and biosorption isotherms

The interaction between Al^{3+} and sorbent (beads containing non-viable biomass) was analyzed using the isotherm models of Langmuir (1918) and Freundlich (1906). Fig. 3 shows the amount of Al^{3+} adsorbed onto beads (q_e(mg/g)) versus the concentration of metal in liquid phase at equilibrium (C_e(mg/L)), as well as the data for both isotherm models fitted to predict the adsorption of Al^{3+} onto beads. Taking into account the results of the adsorption kinetic assays (Fig. 2), for these experiments we selected an equilibration period of 45 min with different metal concentrations (from 0 to 5.4 mg/L Al^{3+}). The experimental data showed that with an increase in metal concentration, adsorption capacity (q_e) increased and saturation was obtained with approximately 0.050 mg Al^{3+}/g beads. This result is in agreement with previous findings which indicate

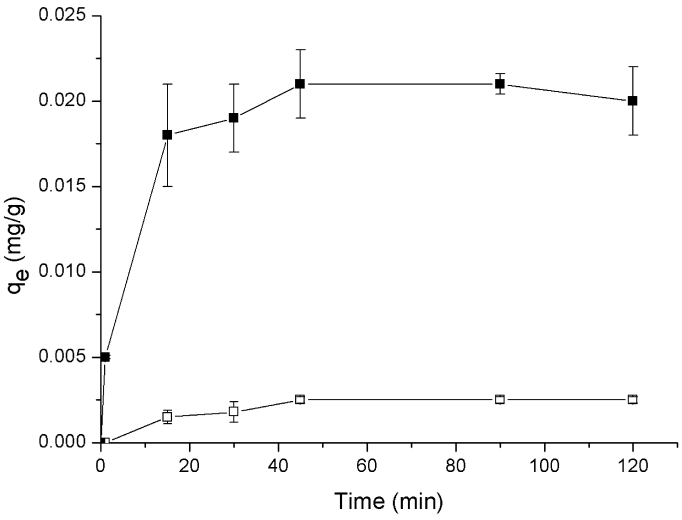

Fig. 2. Effect of contact time on Al^{3+} adsorption capacity of beads with entrapped biomass (■) or empty (□) (Beads: 0.6 g, Al^{3+}: 2.7 mg/L, room temperature, pH: 4.3). Values are means ± SD ($n = 3$).

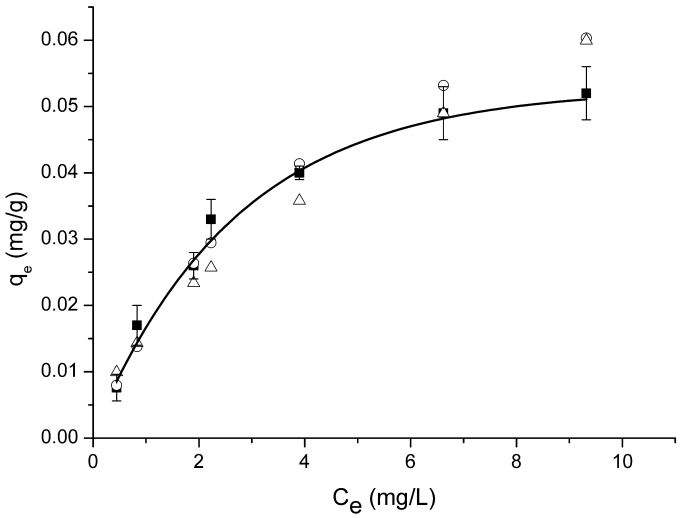

Fig. 3. Adsorption isotherm of Al^{3+} by beads with entrapped biomass (■) experimental data, (○) Langmuir model, (△) Freundlich model. (Beads: 0.15 g, contact time: 45 min, room temperature, pH: 4.3). Values are means ± SD ($n = 3$).

that adsorption capacity is strongly affected by metal concentration in liquid phase, since the ions in the solution act as an important driving force to overcome the resistance to mass transfer between the aqueous and the solid phase (Loutseti et al., 2009; Rashid et al., 2016). Thus, as metal concentration increases, resistance to mass transfer on beads decreases and the metal ions may occupy the available binding sites in the adsorbent until saturation is reached.

The parameters of the Langmuir (q_{max} and K_L) and Freundlich (n and K_F) isotherm models and the coefficients of correlation (R^2) are shown in Table 1. Correlation coefficient values (R^2) indicate that the Langmuir model is a better fit to predict the adsorption of Al^{3+} onto beads with entrapped biomass. Consequently, as described by the Langmuir isotherm, it is possible to assume that adsorption occurs in monolayer. Furthermore, the adsorbent surface has a specific number of sites where adsorption occurs (Vijayaraghavan and Yun, 2008; Xu et al., 2013; Rashid et al., 2016). According to the Langmuir model, the maximum sorption capacity (q_{max}) of the beads was 0.09 mg Al^{3+}/g beads (Table 1), a higher value than the one determined experimentally (0.05 mg Al^{3+}/g beads).

3.1.3. Adsorption/desorption cycles

The efficiency of reusing beads with entrapped biomass was tested for several cycles of adsorption/desorption. Each successive desorption assay lasted 30 min and after eight successive desorption cycles using HCl 0.01 N, the percentage of

Table 1
Parameters of the Langmuir and Freundlich isotherm models for Al^{3+} adsorption onto beads with entrapped biomass.

Langmuir isotherm		Freundlich isotherm	
q_{max} (mg/g)	0.09	n (mg/g)	1.69
K_L (L/mg)	0.218	K_F (L/g)	0.016
R^2	0.97	R^2	0.92

q_{max} = maximum sorption capacity (mg Al^{3+}/g beads), and K_L = Langmuir constant, n = constant related to adsorption intensity, K_F = Freundlich constant, R^2 = regression coefficient.

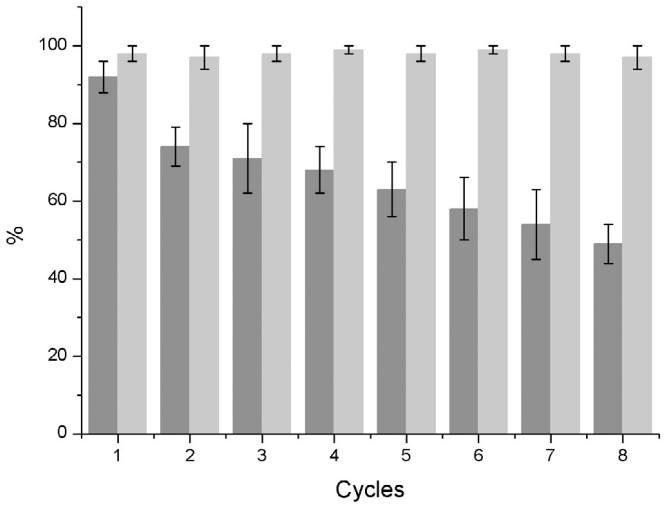

Fig. 4. Adsorption/desorption cycles in batch assay. Dark gray bars: adsorption percentage, light gray bars: desorption percentage.

Al^{3+} desorbed relative to the amount adsorbed to beads in each cycle reached 100% (Fig. 4). This result clearly indicates that HCl is a suitable eluent, as described by Boeris et al. (2016). In contrast with desorption, the percentage of Al^{3+} adsorbed onto beads was about 90% in the first cycle and it decreased over the cycles, reaching only 50% in the eighth cycle (Fig. 4). These results are consistent with those reported previously using non-living free biomass of *P. putida* A (ATCC 12633), where biomass adsorption capacity decreased remarkably from the second desorption cycle onwards, reaching only 28% in the fourth cycle (Boeris et al., 2016). Again, the lowest decrease in adsorption efficiency detected with the beads in relation to free biomass can be attributed to a protection of the union sites by the entrapment of the biomass. As has been described by other authors, in each desorption step the presence of the acid can affect the binding sites present in the biomass (Vijayaraghavan and Yun, 2008; Boeris et al., 2016).

3.2. Biosorption in fixed-bed column

In order to evaluate the technical achievability of continuous metal adsorption, a fixed-bed column (2 cm of inner diameter) was prepared with 60 g beads with non-viable entrapped biomass (25 cm of bed depth) (Fig. 1). Fixed-bed column performance was evaluated in terms of flow rate, metal concentration at the inlet, metal desorption and reuse of the column.

3.2.1. Effect of flow rate and inlet Al^{3+} concentrations

Fig. 5 shows the breakthrough curves with 180 mg/L Al^{3+} in the influent at two different flow rates (0.5 and 1 mL/min). The different parameters obtained from these curves are shown in Table 2. Higher breakthrough time (T_b) and exhausting time (T_e) were obtained at lower flow rates. At 0.5 mL/min T_b and T_e were 60 and 153 min, respectively, while these times were 35 and 134 min when the flow rate was 1 mL/min. Effluent volume (V_{eff}) was treated until exhausting time and the total amount of Al^{3+} sent to the fixed-bed column (me_{total}) increased at greater flow rates.

For both flow rates used, the adsorption capacity of the column (q_{ec}) and the total amount of adsorbed Al^{3+}(q_{total}) were similar, but the removal percentage (R_c%) was considerably higher when a lower flow rate was used (Table 2). This suggests that removal efficiency is independent of the bioadsorbent mass but dependent on the flow rate. As a whole, the greater removal efficiency obtained can be explained if we take into account that at lower flow rates the residence time of Al^{3+} in the column increases, which favors mass transfer from the liquid medium into the beads and also the interaction of the metal with the bioadsorbent. This allows the metal to stay in the column prior before adsorption equilibrium is attained

Table 2
Breakthrough parameters for various operating conditions of the column.

	Inlet concentration 180 mg/L		Rate flow 0.5 mL/min			Inlet concentration 180 mg/L Rate flow 0.5 mL/min			
	Rate flow (mL/min)		Inlet concentration (mg/L)			Cycle			
	0.5	1	150	180	210	1	3	4	12
T_b (min)	60	35	68	60	57	60	63	60	59
T_e (min)	153	134	160	155	144	155	153	152	154
V_{eff} (mL)	76.50	134	80.00	77.50	72.00	77.50	76.50	76.00	77.00
me_{total} (mg)	13.94	24.42	12.00	13.94	15.20	13.95	13.77	13.68	13.86
q_{total} (mg)	8.96	10.83	7.76	8.96	10.95	9.39	8.90	9.29	9.21
R_c%	64.92	44.34	64.66	64.92	72.00	67.31	60.90	67.90	66.45
q_{ec} mg/g	0.15	0.18	0.12	0.15	0.17	0.156	0.148	0.154	0.153

T_b = breakthrough time, T_e = exhausting time, V_{eff} = volume effluent, me_{total} = total amount Al^{3+} sent to the column, q_{total} = total amount of adsorbed Al^{3+}, R_c% = removal percentage of metal, q_{ec} = biosorption capacity of the column (mg Al^{3+}/g beads).

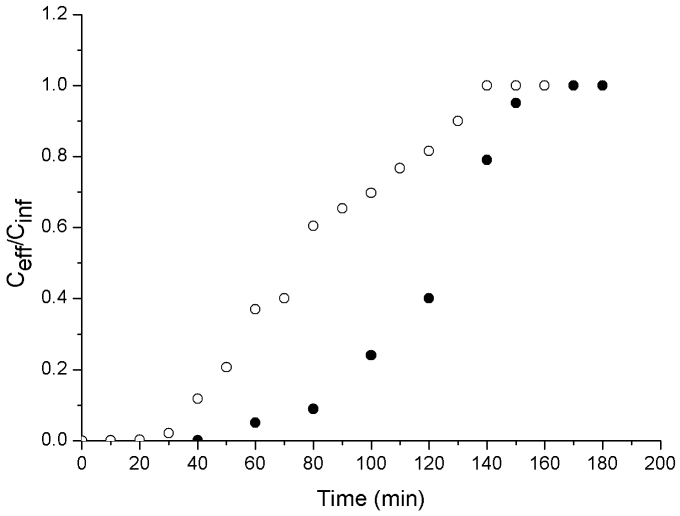

Fig. 5. Breakthrough curve with 180 mg/L of Al^{3+} in the influent at flow rate of 0.5 mL/min (•) and 1 mL/min (○).

(Vijayaraghavan and Yun, 2008; Abdolali et al., 2017; Zang et al., 2017). On the other hand, when the column was prepared with beads without biomass (control), the removal percentage of 180 mg/L Al^{3+} in the influent at a flow rate of 0.5 mL/min was about 10 times lower than that obtained with trapped biomass (not shown). This indicates once again, as was determined in batch (Section 3.1.1), that the presence of non-viable biomass notably increases the availability of binding sites for the cation.

The effect of the adsorption of different initial concentrations of aluminum (150, 180 and 210 mg/L) was evaluated at a flow rate of 0.5 mL/min. With increased inlet metal concentrations, T_b and T_e decreased (Table 2, columns 5, 6 and 7). Thus, at a high metal concentration there was a greater concentration gradient and smaller mass transfer resistance, in such a way that the adsorbent reached saturation more quickly (Abdolali et al., 2017; Zang et al., 2017). The values of me_{total}, q_{total} and q_{ec} increased slightly at high metal concentrations. However, removal percentage (R_c%) was similar for the three concentrations tested, again indicating that metal ions may occupy the available binding sites in the adsorbent until saturation is reached. It should be noted that the sorption capacity of the column is greater than the values obtained experimentally and predicted by the Langmuir isotherm in batch assays (q_{ec} = 0.15 and 0.09 mg Al^{3+}/g beads, respectively). This occurs because packing the adsorbent with a good distribution of immobilized biomass deep down the column favors the interaction of the metal with the bioadsorbent, providing a greater amount of available attachment sites for adsorption (Barquilha et al., 2017). In addition, the presence of ions Na^+, K^+, Ca^{2+}, Cl^-, and SO_4^{2-} at concentrations commonly found in nature (1.3–3.0 g/L) did not detectably interfere with the adsorption of 180 mg/L Al^{3+} in the influent at a flow rate of 0.5 mL/min (data not shown).

3.2.2. Regeneration and reuse of fixed-bed column

The elution of the metal attached to the column after the column bed had been saturated was carried out using different HCl solutions at different flow rates (Table 3). In all conditions evaluated, elution efficiency (E_d) was 100%. At low flow rates, the required time (t_{total}) to achieve 100% elution was higher than those determined for higher flow rates. At flow rates of 0.5 mL/min, V_{elu} and t_{total} values were independent of HCl concentration (0.01 N and 0.1 N). Although at a flow rate of 1 mL/min t_{total} is considerably lower, V_{elu} is greater than 0.5 mL/min.

Table 3
Elution parameters of Al^{3+} ions attached to fixed-bed column.

Rate flow (mL/min)	0.1		0.5		1
HCl (N)	0.01	0.1	0.01	0.1	0.01
E_d%	100	100	100	100	100
t_{total} (min)	2000	2000	400	400	240
V_{elu} (mL)	200	200	200	200	240

E_d = elution efficiency, t_{total} = time until a residual Al^{3+} concentration in the effluent of 99%, V_{elu} = volume of the eluent to desorb 99% of the metal bound onto beads

Table 4
Thomas model constants for Al^{3+} biosorption in a fixed-bed column.

	Inlet concentration 180 mg/L		Rate flow 0.5 mL/min			Inlet concentration 180 mg/L Rate flow 0.5 mL/min			
	Rate flow (mL/min)		Inlet concentration (mg/L)			Cycle			
	0.5	1	150	180	210	1	3	4	12
K_{Th} ($\times 10^{-4}$ L/mg min)	3.78	3.25	4.00	3.78	2.70	2.77	3.72	3.30	3.00
q_0 (mg/g)	0.156	0.190	0.148	0.156	0.212	0.160	0.157	0.176	0.169
R^2	0.97	0.97	0.97	0.97	0.98	0.96	0.97	0.96	0.96

K_{Th} = kinetic constant of Thomas, q_0 = maximum solid-phase concentration of the metal (mg Al^{3+}/g beads), R^2 = regression coefficient.

After each desorption operation the column was washed with deionized water and new adsorptions were carried out (flow rate of 0.5 mL/min and 180 mg/L inlet Al^{3+} concentration). The column system was tested for 12 adsorption/desorption cycles. The parameters determined from breakthrough curves for cycles 1, 3, 4 and 12 are shown in Table 2 (columns 7 to 10). Breakthrough time (T_b), exhausting time (T_e), amount of adsorbed Al^{3+}(q_{total}), biosorption capacity of the column (q_{ec}) and metal removal percentage (R_c%) were practically constant during the 12 cycles, which is evidence of the stability of the adsorbent.

3.2.3. Modeling of breakthrough curves

The successful design of a biosorption column requires the prediction of the breakthrough curves and the maximum capacity of the adsorbent. Two mathematical models were used to predict the dynamic behavior of the column: Thomas (1948) and Yoon and Nelson (1984). The coefficient of correlation (R^2) was better with the Thomas model. This model assumes the Langmuir isotherm and a rate-driving force that obeys second-order reversible reaction kinetics (Xu et al., 2013; Muñoz et al., 2016). The calculated parameters of the Thomas model derived from the experimental data are shown in Table 4. Values for q_0 (mg/g) (maximum solid-phase metal concentration) determined in terms of flow rate, metal concentration at the inlet and reuse of adsorbent were similar to experimental q_{ec} values (Table 2). This means that the Thomas model is suitable for describing Al^{3+} biosorption using beads with entrapped bacterial biomass in a fixed-bed column (Quintelas et al., 2013).

4. Conclusions

Non-viable *P. putida* immobilized in agar–agar was efficient in removing Al^{3+} in batch and continuous column experiments. While the use of immobilized biomaterials for the removal of metals is not novel, this is the first report where the bacterial biomass was immobilized in an economical support, packed in a column and used efficiently to eliminate Al^{+3} from aqueous solutions. Adsorption capacity was higher for the fixed-bed column than for batch assays, suggesting that packing favors the interaction between Al^{3+} and the adsorbent. The flow rate influenced the removal percentage. At high flow rates, residence time of Al^{3+} in the column was lower, in turn decreasing the removal percentage. The results support the notion that the packed bed column developed with *P. putida* biomass immobilized in agar–agar has a high potential for use in the biosorption process for the removal of Al^{3+} from aqueous solutions.

Acknowledgments

GIL, PSB and ASL are Career Members of the Consejo Nacional de Investigaciones Científicas y Técnicas (CONICET). This work was supported by grants from FONCyT (PICT-2013-1475), SECYT–UNRC (PPI: 18/C412) and CONICET (PIP: 11220100100212CO) of Argentina.

Declarations of conflicts of interest

None

References

Abdolali, A., Ngo, H.H., Guo, W., Zhou, J.L., Du, B., Wei, Q., Wang, X.C., Nguyen, P.D., 2015. Characterization of a multi-metal binding biosorbent: Chemical modification and desorption studies. Bioresour. Technol. 193, 477–487.

Abdolali, A., Ngo, H.H., Guo, W., Zhou, J.L., Zhang, J., Liang, S., Chang, S.W., Nguyen, D.D., Liu, Y., 2017. Application of a breakthrough biosorbent for removing heavy metals from synthetic and real wastewaters in a lab-scale continuous fixed-bed column. Bioresour. Technol. 229, 78–87.

Auger, C., Han, S., Appanna, V.P.S., Thomas, C., Ulibarri, G., Appanna, V.D., 2013. Metabolic reengineering invoked by microbial systems to decontaminate aluminum: Implications for bioremediation technologies. Biotechnol. Adv. 31, 266–273.

Barquilha, C.E.R., Cossich, E.S., Tavares, C.R.G., Silva, E.A., 2017. Biosorption of nickel (II) and copper(II) ions in batch and fixed-bed columns by free and immobilized marine algae *Sargassum* sp. J. Cleaner Prod. 150, 58–64.

Boeris, P.S., Agustín, M.R., Acevedo, D.F., Lucchesi, G.I., 2016. Biosorption of aluminum through the use of non-viable biomass of *Pseudomonas putida*. J. Biotechnol. 236, 57–63.

Boeris, P.S., Lucchesi, G.I., 2012. The phosphatidylcholine synthase of Pseudomonas putida A ATCC 12633 is responsible for the synthesis of phosphatidylcholine, which acts as a temporary reservoir for Al^{3+}. Microbiol. 158, 1249–1257.

Buratti, M., Valla, C., Pellegrino, O., Rubino, F.M., Colombi, A., 2006. Aluminum determination in biological fluids and dialysis concentrates via chelation with 8-hydroxyquinoline and solvent extraction/fluorimetry. Anal. Biochem. 353, 63–68.

de Amorim, F.R., Bof, C., Franco, M.B., da Silva, J.B.B., Nascentes, C.C., 2006. Comparative study of conventional and multivariate methods for aluminum determination in soft drinks by graphite furnace atomic absorption spectrometry. Microchem. J. 82, 168–173.

Devaraj, M., Saravanan, R., Deivasigamani, R., Gupta, V.K., Gracia, F., Jayadevan, S., 2016. Fabrication of novel shape Cu and Cu/Cu_2O nanoparticles modified electrode for the determination of dopamine and paracetamol. J. Mol. Liq. 221, 930–941.

Dhanarani, S., Viswanathan, E., Piruthiviraj, P., Arivalagan, P., Kaliannan, T., 2016. Comparative study on the biosorption of aluminum by free and immobilized cells of *Bacillus safensis* KTSMBNL 26 isolated from explosive contaminated soil. J. Taiwan. Inst. Chem. Eng. 69, 61–67.

Dhoble, R.M., Maddigapu, P.R., Rayalu, S.S., Bhole, A.G., Dhoble, A.S., Dhoble, S.R., 2017. Removal of arsenic(III) from water by magnetic binary oxide particles (MBOP): Experimental studies on fixed bed column. J. Hazard. Mater. 322, 469–478.

Dixon, E.M., 1997. Proposed environmental quality standards for aluminium in water. Environment Agency R&D Note EA 4218 WRc Medmenham, p. 90.

Errasquin, E.L., Vazquez, C., 2003. Tolerance and uptake of heavy metals by *Trichoderma atroviride* isolated from sludge. Chemosphere 50, 137–143.

Febrianto, J., Kosasih, A.N., Sunarso, J., Ju, Y., Indraswati, N., Ismadji, S., 2009. Equilibrium and kinetic studies in adsorption of heavy metals using biosorbent: a summary of recent studies. J. Hazard. Mater. 162, 616–645.

Freundlich, H., 1906. Ueber die adsorption in loesungen. Z. Phis. Chem. 57, 385–470.

Garcidueñas Piña, R., Cervantes, C., 1996. Microbial interactions with aluminium. Biol. Met. 9, 311–316.

Gupta, V.K., Nayak, A., 2012. Cadmium removal and recovery from aqueous solutions by novel adsorbents prepared from orange peel and Fe_2O_3 nanoparticles. Chem. Eng. J. 180, 81–90.

Hejri, O.M., Bzogzadeh, E., Soleimani, M., Mozaheri, R., 2011. Determination of trace aluminum with eriochromecyanine R after cloud point extraction. World Appl. Sci. J. 15, 218–222.

Kochian, L.V., Pineros, M.A., Hoekenga, O.A., 2005. The physiology, genetics and molecular biology of plant aluminum resistance and toxicity. Plant Soil 274, 175–195.

Kumari, A.A., Ravindhranath, K., 2012. Removal of aluminium (III) from polluted waters using biosorbents derived from *Achiranthusaspera* and *Cassia occidentalis*. Int. J. Water Resour. Environ. Sci. 1, 8–19.

Langmuir, I., 1918. The adsorption of gases on plane surfaces of glass, mica and platinium. J. Am. Chem. Soc. 40, 1361–1403.

Loutseti, S., Danielidis, D.B., Economou-Amilli, A., Katsaros, Ch., Santas, R., Santas, Ph., 2009. The application of a micro-algal/bacterial biofilter for the detoxification of copper and cadmium metal wastes. Bioresour. Technol. 100, 2099–2105.

Mailloux, R.J., Lemire, J., Appanna, V.D., 2011. Hepatic response to aluminum toxicity: dyslipidemia and liver diseases. Exp. Cell Res. 317, 2231–2238.

Majumder, S., Gangadhar, G., Raghuvanshi, S., Gupta, S., 2015. Biofilter column for removal of divalent copper from aqueous solutions: Performance evaluation and kinetic modeling. J. Water Process Eng. 6, 136–143.

Mittal, A., Mittal, J., Malviya, A., Kaur, D., Gupta, V.K., 2010. Decoloration treatment of a hazardous triarylmethane dye, Light Green SF (Yellowish) by waste material adsorbents. J. Colloid Interface Sci. 342, 518–527.

Mokaddem, H., Azouaou, N., Kaci, Y., Sadaoui, Z., 2014. Study of lead adsorption from aqueous solutions on agar beads with EPS produced from *Paenibacilluspolymyxa*. Chem. Eng. Trans. 38, 31–36.

Muñoz, A.J., Espínola, F., Ruiz, E., 2016. Removal of Pb(II) in a packed-bed column by a *Klebsiella* sp. 3S1 biofilm supported on porous ceramic Raschig rings. J. Ind. Eng. Chem. 40, 118–127.

Muñoz, A.J., Espínola, F., Ruiz, E., 2017. Biosorption of Ag(I) from aqueous solutions by *Klebsiella* sp. 3S1. J. Hazard. Mater. 329, 166–177.

Palleroni, N.J., 1992. Taxonomy and Identification. In: Galli, E., Silver, S., Witholt, B. (Eds.), *Pseudomonas*, Molecular Biology and Biotechnology. DC: American Society for Microbiology, Washington, pp. 105–115.

Quintelas, C., Pereira, R., Kaplan, E., Tavares, T., 2013. Removal of Ni(II) from aqueous solutions by an *Arthrobacterviscosus* biofilm supported on zeolite: from laboratory to pilot scale. Bioresour. Technol. 142, 368–374.

Rashid, A., Bhatti, H.N., Iqbal, M., Noreen, S., 2016. Fungal biomass composite with bentonite efficiency for nickel and zinc adsorption: A mechanistic study. Ecol. Eng. 91, 459–471.

Singh, S., Tripathi, D.K., Singh, S., Sharma, S., Dubey, N.K., Chauhan, D.K., Vaculík, M., 2017. Toxicity of aluminium on various levels of plant cells and organism: a review. Environ. Exp. Bot. 137, 177–193.

Soylak, M., Sahin, U., Ulgen, A., Elci, L., Dogan, M., 1997. Determination of aluminum at trace level in water samples by visible absorption spectroscopy with a laser diode. Anal. Sci. 13, 287–289.

Sukweenadhi, J., Kim, Y.J., Choi, E.S., Koh, S.C., Lee, S.W., Kim, Y.J., Yang, D.C., 2015. *Paenibacillus yonginensis* DCY84 T induces changes in *Arabidopsis thaliana* gene expression against aluminum, drought, and salt stress. Microbiol. Res. 172, 7–15.

Tassist, A., Lounici, H., Abdi, N., Mameri, N., 2010. Equilibrium, kinetic and thermodynamic studies on aluminum biosorption by a mycelial biomass (*Streptomyces rimosus*). J. Hazard. Mater. 183, 35–43.

Tharmalingam, S., Alhasawi, A., Appanna, V.P., Appanna, V.D., 2007. Decontamination of multiple-metal pollution by microbial systems: the metabolic twist. In: Das, S., Dash, H.R. (Eds.), Handbook of Metal-Microbe Interactions and Bioremediation. CRC Press, Boca Raton, New York, pp. 151–172.

Thomas, H.G., 1948. Chromatography: a problem in kinetics. Ann. New York Acad. Sci. 49, 161–182.

Tomljenovic, L., 2011. Aluminum and Alzheimer's disease: after a century of controversy, is there a plausible link? J. Alzheimers Dis. 23, 567–598.

Tuzen, M., Soylak, M., 2008. Biosorption of aluminium on *Pseudomonas aeruginosa* loaded on Chromosorb 106 prior to its graphite furnace atomic absorption spectrometric determination. J. Hazard. Mater. 154, 519–525.
Vijayaraghavan, K., Yun, Y.S., 2008. Bacterial biosorbents and biosorption. Biotechnol. Adv. 26, 266–291.
Wang, J., Chen, C., 2009. Biosorbents for heavy metals removal and their future. Biotechnol. Adv. 27, 195–226.
Wong, M.H., Zhang, Z.Q.J., Wong, W.C., Lan, C.Y., 1998. Trace metal contents (Al, Cu and Zn) of tea: tea and soil from two tea plantations, and tea products from different provinces of China. Environ. Geochem. Health. 20, 87–94.
Xu, Z., Cai, J.G., Pan, B.C., 2013. Mathematically modeling fixed-bed adsorption in aqueous systems. J. Zhejiang Univ. Sci. A 14, 155–176.
Yoon, Y.H., Nelson, J.H., 1984. Application of gas adsorption kinetics I. A theoretical model for respirator cartridge service life. Am. Ind. Hyg. Assoc. J. 45, 509.
Zang, T., Cheng, Z., Lu, L., Jin, Y., Xu, X., Ding, W., Qu, J., 2017. Removal of Cr(VI) by modified and immobilized *Auricularia auricular* spent substrate in a fixed-bed column. Ecol. Eng. 99, 358–365.